Application of Trajectory Surface Hopping to the Study of a Symmetry-Forbidden Intramolecular Hole Transfer Process in Bismethyleneadamantane Cation Radical

Garth A. Jones, Barry K. Carpenter,*,[1] and Michael N. Paddon-Row*

Contribution from the School of Chemistry, University of New South Wales, Sydney 2052, Australia

Received May 28, 1999. Revised Manuscript Received September 24, 1999

Abstract: A recently developed, Landau−Zener-based quasiclassical trajectory surface-hopping method for medium-sized organic molecules is used to investigate hole transfer (HT) in the formally symmetry forbidden hole transfer process in bismethyleneadamantane cation radical **4a** and its d_4-labeled analogue **4b**. The calculations involve sets of 200 trajectories, sampled from a canonical ensemble at 298.15 K, to directly calculate the mean first passage times, τ, for HT in both systems, together with Fourier transform analyses to identify the important modes which induce hole transfer. Very small τ values for hole transfer are predicted, despite the fact that the reaction is nominally symmetry forbidden. The main symmetry breaking mode is identified as the torsional vibration about the terminal methylene group on the one-electron, π bond. An approximate secondary kinetic isotope effect is calculated, and is shown to be largely attributable to the change in frequency of the key torsional mode. The magnitude of the electronic coupling at the avoided crossing region for HT in both **4a** and **4b** is estimated to be 0.01 eV, placing the HT process within the nonadiabatic regime. It is found that qualitatively, the calculated τ values and the derived approximate secondary kinetic isotope effects are fairly insensitive to the method used to identify the avoided crossing region in the trajectory calculations. It is concluded that the trajectory surface-hopping method described herein should provide useful qualitative insights into the effect of nuclear dynamics on ET and HT processes occurring in a variety of structurally complex systems of chemical interest.

I. Introduction

Much progress has been made in our understanding of the mechanism of long-range electron transfer (ET) and hole transfer (HT) processes.[2] In particular, experimental studies using novel, structurally well-defined multichromophoric systems have provided a wealth of data on the effect of distance,[3] orientation,[4] solvent,[5] driving force,[6] and orbital symmetry[7] on the dynamics of ET and HT processes. These data have been used to verify salient predictions of several important theoretical models of ET and HT.

Traditionally, charge-transfer processes are described by the mixing of two diabatic surfaces, one representing the electronic configuration of the reactant, and the other representing the configuration of the product. In the region where the diabatic surfaces approach each other, mixing of these diabatic configurations gives rise to an avoided crossing, the magnitude of which is twice the value of the electronic coupling matrix element V_{el} at this point.[8] In the case of weak nonadiabatic coupling, the ET rate constant k_{et} may be obtained from the Fermi golden rule, eq 1, where FCWD is the Franck−Condon weighted density of states. The quadratic dependence of k_{et} on V_{el} is a central relationship in ET theory.[9]

$$k_{et} = \frac{4\pi^2}{h}|V_{el}|^2\mathrm{FCWD} \qquad (1)$$

A pivotal problem in nonadiabatic ET theory is the determination of the magnitude of the electronic coupling matrix element, V_{el}, and how its magnitude depends on structural and environmental factors. To date, this information has come about

(1) Permanent address: Department of Chemistry and Chemical Biology, Baker Laboratory, Cornell University, Ithaca, NY 14853-1301.

(2) (a) Paddon-Row, M. N. *Acc. Chem. Res.* **1994**, *27*, 18 and references therein. (b) Wasielewski, M. R. *Chem. Rev.* **1992**, *92*, 435. (c) Closs, G. L.; Miller, J. R. *Science* **1988**, *240*, 440. (d) Barbara, P. F.; Meyer, T. J.; Ratner, M. A. *J. Phys. Chem.* **1996**, *100*, 13148.

(3) (a) Paddon-Row, M. N.; Verhoeven, J. W. *New J. Chem.* **1991**, *15*, 107 and references therein. (b) Oevering, H.; Paddon-Row, M. N.; Heppener, M.; Oliver, A. M.; Cotsaris, E.; Verhoeven, J. W.; Hush, N. S. *J. Am. Chem. Soc.* **1987**, *109*, 3258. (c) Joran, A. D.; Leland, B. A.; Geller, G. G.; Hopfield, J. J.; Dervan, P. B. *J. Am. Chem. Soc.* **1984**, *106*, 6090. (d) Hush, N. S.; Paddon-Row, M. N.; Cotsaris, E.; Oevering, H.; Verhoeven, J. W.; Heppener, M. *Chem. Phys. Lett.* **1985**, *117*, 8. (e) Johnson, M. D.; Miller, J. R.; Green, N. S.; Closs, G. L. *J. Phys. Chem.* **1989**, *93*, 1173.

(4) Knapp, S.; Dhar, T. G. M.; Albaneze, J.; Gentemann, S.; Potenza, J. A.; Holten, D.; Schugar, H. J. *J. Am. Chem. Soc.* **1991**, *113*, 4016.

(5) (a) Clayton, A. H. A.; Ghiggino, K. P.; Lawson, J. M.; Paddon-Row, M. N. *J. Photochem. Photobiol. A: Chem.* **1994**, *80*, 323. (b) Roest, M. R.; Verhoeven, J. W.; Schuddeboom, W.; Warman, J. M.; Lawson, J. M.; Paddon-Row, M. N. *J. Am. Chem. Soc.* **1996**, *118*, 1762.

(6) (a) Calcaterra, L. T.; Closs, G. L.; Miller, J. R. *J. Am. Chem. Soc.* **1983**, *105*, 670. (b) Miller, J. R.; Calcaterra, L. T.; Closs, G. L. *J. Am. Chem. Soc.* **1984**, *106*, 3047.

(7) (a) Oliver, A. M.; Paddon-Row, M. N.; Kroon, J.; Verhoeven, J. W. *Chem. Phys. Lett.* **1992**, *191*, 371. (b) Reimers, J. R.; Hush, N. S.; Sammeth, D. M.; Callis, P. R. *Chem. Phys. Lett.* **1990**, *169*, 622. (c) Zeng, Y.; Zimmt, M. B. *J. Am. Chem. Soc.* **1991**, *113*, 5107.

(8) (a) Bolton, J. R.; Archer, M. D. In *Electron Transfer in Inorganic, Organic and Biological Systems*; Bolton, J. R., Mataga, N., McLendon, G. L., Eds.; Advances in Chemistry Series 228; American Chemical Society: Washington, DC, 1991; Chapter 2, pp 7−23. (b) Paddon-Row, M. N.; Jordan, K. D. In *Modern Models of Bonding and Delocalisation*; Liebman, J. F., Greenberg, A. Eds.; VCH Publishers Inc.: New York, 1988; Chapter 3. (c) Jordan, K. D.; Paddon-Row, M. N. *Chem. Rev.* **1992**, *92*, 395.

(9) (a) Mikkelsen, K. V.; Ratner, M. A. *Chem. Rev.* **1987**, *87*, 113 and references therein. (b) Levich, V. G. *Adv. Electrochem. Eng.* **1966**, *4*, 249. (c) Sutin, N.; Marcus, R. A. *Biochim. Biophys. Acta* **1985**, *811*, 256.

10.1021/ja9917823 CCC: $18.00
Published on Web 11/17/1999

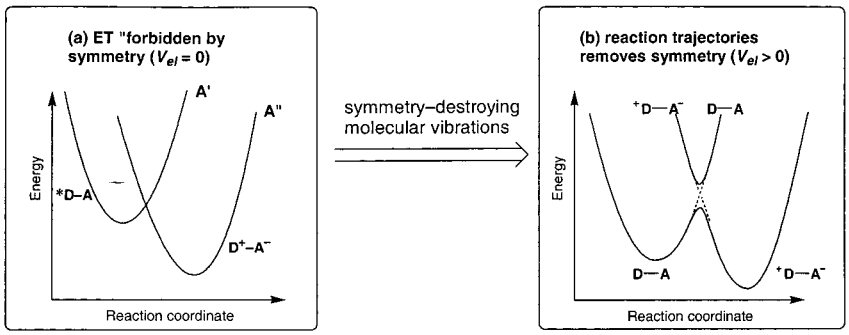

Figure 1. Photoinduced ET proceeding from the locally excited state of the donor (*D) to the acceptor (A). (a) Symmetries of the reactant and product states are different in the vibrationless case and $V_{el} = 0$. (b) Certain vibrational modes destroy the symmetry, making V_{el} nonzero. (The ground-state surface is not shown.)

from static models in which the explicit dynamic effects of molecular vibrations are ignored. Although it is true that, within the context of nonadiabatic ET theories, molecular vibrations are incorporated into the Franck−Condon factor as a probability of the system reaching the transition structure for ET, these theories fail to address several important issues concerning donor-bridge-acceptor systems. These include the following: (1) Which molecular vibrations are responsible for mediating the ET process? (2) What effect do *bridge* vibrations have on the magnitude of V_{el}? (3) How is the electronic coupling element V_{el} affected by molecular vibrations of the *chromophores?*

That molecular vibrations markedly influence the magnitude of the electronic coupling, V_{el}, and hence the dynamics of ET and HT processes is dramatically illustrated by considering ET processes that are formally forbidden on the grounds of state symmetry. We present three examples, namely photoinduced ET in the bichromophoric systems **1** and **2**, and rapid excitation

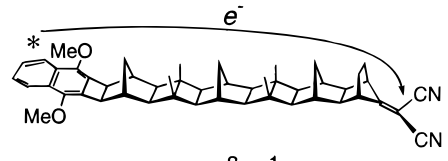

1 ● k_{et} = 1.2 x 10^8 s^{-1}

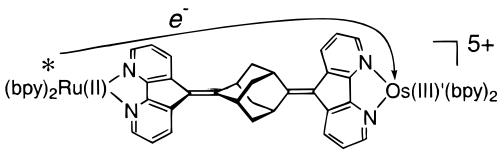

2 ● k_{et} = 8.3 x 10^8 s^{-1}

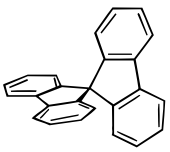

3 ● k_{EET} ~ 1 x 10^{12} s^{-1}

energy transfer between the orthogonal chromophores of the spirane system **3**. Electron transfer in **1** occurs from the locally excited singlet state of the dimethoxnaphthalene (DMN) donor to the dicyanovinyl (DCV) acceptor. Within the context of C_s point group symmetry, the lowest excited singlet state of **1** has A′ symmetry, whereas the charge separated product state has A″ symmetry. The electronic coupling for the ET process occurring under C_s symmetry constraint is therefore zero (Figure 1a). The electronic coupling for photoinduced ET in **2** should likewise be zero, if this system retains local D_{2d} symmetry within the bismethyleneadamantane unit. However, the experimental photoinduced intramolecular ET rates in these systems are extremely rapid, $>10^8$ s^{-1} in both cases.[2a,3b,7a,10a] Clearly, certain vibrational motions (vibronic coupling) in these systems remove the offending symmetry constraint, and lead to a substantial magnitude of V_{el} (Figure 1b).[7b] Formally symmetry forbidden excitation energy transfer (EET) processes may also take place rapidly as a result of vibronic coupling. Thus, Yip et al. have observed rapid EET ($> 10^{12}$ s^{-1}) taking place in systems based on **3**.[10b] Intriguing questions then arise from these experimental data, such as the following: Is there more than one vibrational mode responsible for generating strong electronic coupling? Which modes are primarily responsible for producing the coupling? Answers to these questions are amenable to experimental verification through judicious use of isotopic labeling.

Recently, we have described a molecular dynamics (MD) model,[11] which incorporates the trajectory surface hopping (TSH) method (MD-TSH),[12] that shows promise in answering a number of important questions in ET, including those mentioned above. In this paper, we apply this model to computing the molecular dynamics of HT for the bismethyleneadamantane cation radical systems, **4a** and **4b**, which serve

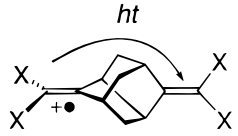

4 **a: X = H**
b: X = D

as simple models for **2**. The layout of this paper is as follows.

(10) (a) De Cola, L.; Balzani, V.; Barigelletti, F.; Flamigni, L.; Belser, P.; Bernhard, S. *Recl. Trav. Chim. Pays-Bas* **1995**, *114*, 534. (b) Yip, W. T.; Levy, D. H.; Kobetic, R.; Poitrowiak, P. *J. Phys. Chem. A* **1999**, *103*, 10.

(11) Jones, G. A.; Carpenter, B. K.; Paddon-Row, M. N. *J. Am. Chem. Soc.* **1998**, *120*, 5499.

(12) (a) Preston, R. K.; Tully, J. C. *J. Chem. Phys.* **1971**, *54*, 4297. (b) Tully, J. C.; Preston, R. K. *J. Chem. Phys.* **1971**, *55* 562. (c) Miller, W. H.; George, T. F. *J. Chem. Phys.* **1972**, *56*, 5637. (d) Tully, J. C. *Ber. Bunsen-Ges. Phys. Chem.* **1973**, *77*, 557. (e) Stine, J. R.; Muckerman, J. T. *J. Chem. Phys.* **1976**, *65*, 3975. (f) Tully, J. C. In *Dynamics of Molecular Collisions, Part B*; Miller, W. H., Ed.; Plenum: New York, 1976; p 217. (g) Kuntz, P. J.; Kendrick, J.; Whitton, W. N. *Chem. Phys.* **1979**, *38*, 147. (h) Blais, N. C.; Truhlar, D. G. *J. Chem. Phys.* **1983**, 79, 1334. (i) Parlant, G.; Gisalson, E. A. *J. Chem. Phys.* **1989**, *91*, 4416. (j) Mead, C. A.; Truhlar, D. G. *J. Chem. Phys.* **1986**, *84*, 1055. (k) Stine, J. R.; Muckerman, J. T. *J. Chem. Phys.* **1986**, *84*, 1056. (l) Chapman, S. *Adv. Chem. Phys.* **1992**, *82*, 423.

First, we present a brief description of our MD-TSH model. The mean first passage times for HT at 298.15 K in **4a** and in the d_4-labeled system, **4b**, τ_h and τ_d, respectively, are estimated. Fourier transforms of reaction trajectories are used to identify important vibrational modes that drive the HT process. The modulation of V_{el} by these modes is then analyzed. Finally, approximate kinetic isotope effects are calculated from the calculated τ values for HT in **4a** and **4b**. These provide a basis for experimental verification.

II. The MD-TSH Model

Basic Description. The desire to develop a method that can provide insight into the dynamics of HT or ET in relatively large organic molecules and ions of experimental interest necessarily limits the level of theory that can be employed, and hence the quantitative accuracy of the results to be expected. Our principal purpose in this research is to identify key dynamic features of the HT or ET events that might be masked in the more traditional, nondynamic theories. Since development of an analytical potential energy surface (PES) is entirely impractical for molecules of the size considered here, direct dynamics techniques are mandated. These, in turn, require relatively fast methods for evaluating the potential energy and its derivatives at each time step of an evolving trajectory. We have employed AM1 semiempirical MO theory, with 2×2 CI, for this purpose. In calculations on closed-shell molecules, the accuracy of the AM1 method can be improved by reparametrizing it to fit the results at key points on the PES from high-level ab initio calculations.[13] However, even that level of theory is impractical for studies of radical ions of the kind considered here. The reason is that such ions are susceptible to doublet instability at the Hartree−Fock (HF) level. This artifact makes the energies of symmetrical transition structures spuriously too high. With density functional theories the reverse problem occurs: radical ions are predicted by all of the commonly used functionals to be spuriously symmetrical and delocalized.[14] We have confirmed that both of these errors do occur in the systems of interest to us.[11] Thus, the lowest level of ab initio theory that could plausibly give qualitatively correct PESs for these species would be some kind of MCSCF or CI calculation, but these are currently not computationally tractable for such large ions if a reasonable basis set is employed.

Given this limitation of ab initio theory, we have chosen to employ the AM1[15] method with its original parameters, recognizing that the results of the calculations will necessarily be only qualitatively reliable. It is worth pointing out, however, that the "half-electron" model[16] used in the MOPAC[17] implementation of AM1 appears to avoid both the doublet instability of ab initio HF theory and the "inverse symmetry breaking" of DFT theory.[18]

In the same spirit, we have used the lowest level of nonadiabatic dynamics that could be expected to describe the system properly. Although recent years have seen tremendous strides in the development of nonadiabtic dynamic theories,[19] it seems inappropriate to use highly sophisticated dynamic models on a highly approximate PES. Indeed, it is often the case that qualitative insight into reactivity comes more readily from less sophisticated models.[18,20]

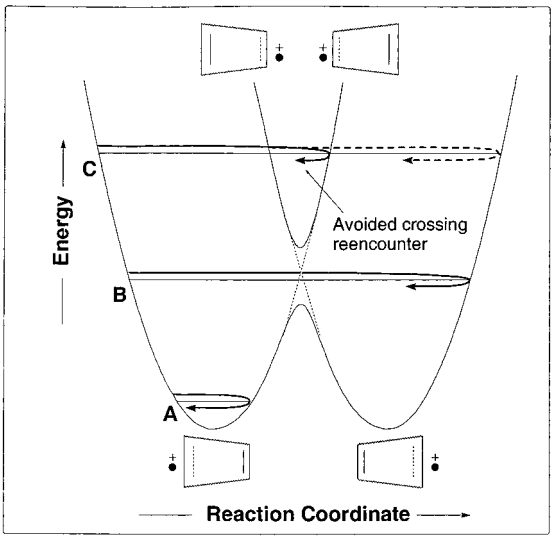

Figure 2. Behavior of various trajectories (curved arrows) on the adiabatic surfaces. For trajectory **A**, the total energy (potential energy plus kinetic energy in the reaction coordinate) is insufficient to surmount the barrier on the lower surface and so hole transfer cannot occur. For trajectory **B**, the total energy is sufficient to cross the barrier on the lower surface but insufficient to provide access to the upper surface. For trajectory **C**, the total energy is sufficient to allow access to the upper surface and so two outcomes are possible. If a transition to the upper electronic state occurs, hole transfer is inhibited, but the system soon encounters a PE barrier that causes it to return rapidly to the region of the avoided crossing. This is shown by the solid curved arrow. If the system stays in the lower electronic state, hole transfer analogous to that for trajectory **B** will occur. This is depicted by the dashed curved arrow.

Our MD-TSH method has been described in detail in the first paper of this series.[11] Briefly, it is based on Tully and Preston's "anteater" approach,[12a,b] and it may be illustrated using the example of hole transfer within a diene cation radical (Figure 2). The two diabatic surfaces mix to form the lower and upper adiabatic surfaces. HT takes place on the lower surface in the avoided crossing region. In this region, the energy gap between the two adiabatic curves, ΔE, is twice the electronic coupling V_{el} for the HT process. The trajectory is started using suitable initial conditions (which include distributing vibrational quanta among the various normal modes). Both lower and upper surfaces are calculated "on the fly" using 2×2 CI (higher order CI could be used if needed). If the trajectory has sufficient kinetic energy in the direction that carries reactant into product (i.e. trajectories B and C of Figure 2), then it will eventually enter the avoided crossing region. At this point the Landau−Zener (LZ) criterion[21] is used to determine whether TSH to the upper surface may take place or not. If TSH does not occur, then the trajectory remains on the lower surface and leads to HT, at which point the run is halted. If TSH is predicted to occur, then the Miller−George criterion[12c] is applied to ascertain whether the trajectory has sufficient energy to make the surface hop (*i.e.* type C) or not (i.e. type B). In the latter event, HT occurs and the run is stopped. On the other hand, if the trajectory is of type C, then TSH to the upper surface occurs, in which case no HT takes place; the trajectory now oscillates about the avoided crossing region on the upper surface. Every time it enters the avoided crossing, the LZ criterion is applied to determine if TSH to the lower surface occurs. If TSH occurs while the trajectory is moving in the direction of the product well, HT takes place and the run is terminated, whereas if the trajectory is moving in the direction of the reactant well, it is continued until HT does occur.

(13) Gonzalez-Lafont, A.; Truong, T. N.; Truhlar, D. G. *J. Phys. Chem.* **1991**, *95*, 4618.

(14) (a) Noodleman, L.; Post, D.; Baerends, E. J. *J. Chem. Phys.* **1982**, *64*, 159. (b) Bally, T.; Sastry, G. N. *J. Phys. Chem. A* **1997**, *101*, 7923. (c) Shephard, M. J.; Paddon-Row, M. N. *Chem. Phys. Lett.* **1999**, *301*, 281.

(15) Dewar, M. J. S.; Zoebisch, E. G.; Healy, E. F.; Stewart, J. J. P. *J. Am. Chem. Soc.* **1985**, *107*, 3902.

(16) (a) Nesbet, R. K. *Proc. R. Soc.* **1955**, *A230*, 312. (b) Dewar, M. J. S.; Hashmall, J. A.; Venier, C. G. *J. Am. Chem. Soc.* **1968**, *90*, 1953.

(17) MOPAC93, Revision 2: Stewart, J. J. P.; Fujitsu: Tokyo, Japan, 1993.

(18) (a) Rauhut, G.; Clark, T. *J. Am. Chem. Soc.* **1993**, *115*, 9127. (b) Rauhut, G.; Clark, T. *J. Chem. Soc., Faraday Trans.* **1994**, *90*, 1783.

(19) (a) Tully, J. C. *J. Phys. Chem.* **1990**, *93*, 1061. (b) Webster, F. A.; Rossky, P. J.; Friesner, R. A. *Comput. Phys. Commun.* **1991**, *63*, 494. (c) Coker, D. F. In *Computer Simulation in Chemical Physics*; Allen, M. P., Tildesley, D. J., Eds.; Kluwer Academic Publishers: Dordrecht, 1993; Vol. 397. (d) Hammes-Schiffer, S.; Tully, J. C. *J. Chem. Phys.* **1994**, *101*, 4657. (e) Hammes-Schiffer, S.; Tully, J. C. *J. Phys. Chem.* **1995**, *99*, 5793. (f) Martinez, T. J.; Levine, R. D. *J. Chem. Soc., Faraday Trans.* **1997**, *93*, 941. (g) Prezhdo, O. V.; Rossky, P. J. *J. Chem. Phys.* **1997**, *107*, 825. (h) Ben-Nun, M.; Martinez, T. J. *J. Chem. Phys.* **1998**, *108*, 7244.

(20) Carpenter, B. K. In *Advances in Molecular Modeling*; Liotta, D., Ed.; JAI Press: Greenwich, CT, 1988.

(21) (a) Landau, L. D. *Phys. Z. Sowjetunion* **1932**, *2*, 46. (b) Zener, C. *Proc. R. Soc. London* **1932**, *A137*, 696.

Information that may be obtained from these runs includes the following: (1) Fourier transform of the energy gap between the upper and lower surfaces versus time for a trajectory enables the identification of the major vibrational modes which are responsible for modulating the electronic coupling for the HT process. (2) Using trajectories sampled from a canonical ensemble of initial states, a plot of the fraction of trajectories remaining after a period of time versus time is used to calculate the mean first passage time for HT.

An important issue in the method is the determination of the reaction seam of avoided crossings at which nonadiabatic events (e.g. TSH) may take place. While the use of direct-dynamics techniques makes the *prior* identification of the explicit location of the PES seam of avoided crossings unnecessary, the choice of when to check for surface hops is not uniquely defined. One could, for example use the beginnings of hole transfer on the lower adiabatic PES (as judged by charge migration) as the criterion (hereafter referred to as Method I), or one could carry out the Landau−Zener calculation every time the plot of energy gap between the two adiabatic surfaces vs time passes through a minimum (hereafter referred to as Method II). Method I was employed in the first paper of the series[11] and it will also be employed here. However, the energy gap associated with the avoided crossing located using this method is generally found to be larger than the minimum value. Consequently, this method gives an inflated value for the electronic coupling V_{el}. In contrast, Method II should give the correct value for V_{el} since the energy gap associated with the avoided crossing, using this method, is a minimum. The sensitivity of our model to the choice of method for locating the avoided crossing seam (Method I vs Method II) will be addressed at the end of the paper.

Generation of Initial States. A canonical ensemble at 298.15 K was generated by quasiclassical normal-mode sampling, using a procedure modified from that of Chapman and Bunker (CB).[22] In the CB method, a harmonic relationship between amplitude and potential energy is assumed for each normal mode, and then corrections for the failures of this relationship that occur with finite displacements from the stationary point are made by an iterative scaling device. In the present procedure, the relationship between displacement and potential energy was fitted to the expression:

$$\Delta E_i = \sum_{j=2}^{5} a_{ij} \xi_i^j \qquad (2)$$

for the *i*th normal mode. ΔE_i is the potential energy in excess of the stationary-point value, ξ_i^j is the displacement along the direction of the normal coordinate, and the a_{ij} are empirically determined coefficients. For the initial states of each of the trajectories in this study, total potential energy above the stationary point due to simultaneous displacements along all of the normal coordinates was found to be within 1 kcal/mol of the MOPAC value when calculated by eq 2.

The number of quanta in excess of the zero point was selected for each normal mode by choosing the largest integer, n_i, to satisfy relationship 3:

$$n_i \leq -\frac{k_B T}{hc\nu_i} \ln(R_{1i}) \qquad (3)$$

where k_B is Boltzmann's constant, h is Planck's constant, c is the speed of light, T is the temperature (here 298.15 K), ν_i is the frequency of the *i*th normal mode (in cm^{-1}), and R_{1i} is a random number in the range $0 < R_{1i} \leq 1$.

The energy in each normal mode, $(n_i + 1/2)hc\nu_i$, was converted to a maximum displacement ξ_i by eq 2, and then the actual displacement, q_i, selected by eq 4:

$$q_i = \xi_i \cos(2\pi R_{2i}) \qquad (4)$$

where R_{2i} is a second random number in the range $0 \leq R_{2i} \leq 1$. Since the maximum displacements at a given energy were typically not symmetrical in the positive and negative directions of the normal-coordinate eigenvector, the value appropriate for the sign of eq 4 was used.

(22) Chapman, S.; Bunker, D. L. *J. Chem. Phys.* **1975**, *62*, 2890.

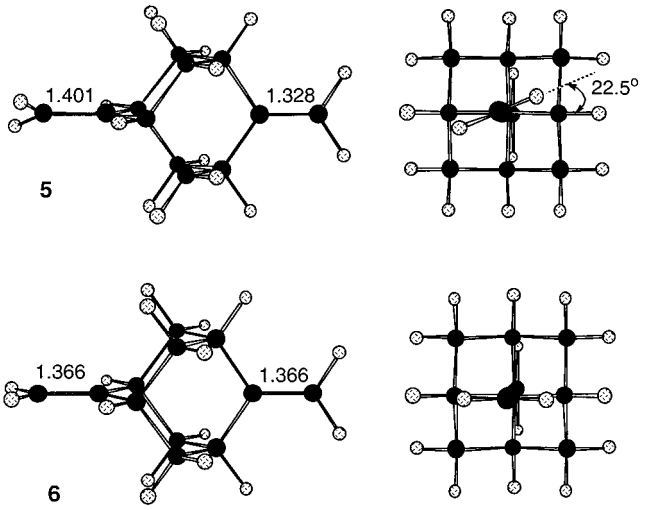

Figure 3. AM1-CI optimized structures for the ground-state global minimum energy C_1 structure, **5**, and the D_{2d} "transition structure", **6**. Depicted bond lengths are in angstroms.

The kinetic energy in each normal mode (the difference between the total energy, $(n_i + 1/2)hc\nu_i$, and the potential energy due to displacement from the stationary point) was used to calculate Cartesian velocity components for each atom, with the directions being selected by a third random number. External molecular rotations were not energized.

The Cartesian atomic coordinates and velocities then formed the input for the dynamic reaction coordinate routine that is part of MOPAC. The trajectories were allowed to run for a maximum of 500 fs (fs) using time intervals of 0.1 fs.

III. Results and Discussion

Ground-State Potential Energy Surface. At the AM1-CI level of theory, the ground-state global minimum energy structure for bismethyleneadamantane cation radical **4a** has C_1 symmetry and the positive charge is formally localized on one of the double bonds, making that double bond essentially a one-electron π bond (structure **5**, Figure 3). Consequently, the two double bonds have unequal lengths, 1.401 and 1.328 Å, corresponding to the one-electron and two-electron π bonds, respectively. The one-electron π bond is twisted by 22.5° about its axis and this is consistent with the fact that the ethene cation radical has been shown, both experimentally and computationally, to exhibit a similar degree of torsion.[23] The cation radical **4a** has a calculated heat of formation of 218.5 kcal/mol. Vertical removal of an electron from the degenerate pair of π MOs of neutral, D_{2d} bismethyleneadamantane produces a charge-delocalized cation radical. As expected, the D_{2d} structure is associated with an electronically degenerate state and the electronic coupling between these states is therefore zero. The system is Jahn−Teller unstable and it is reasonable to assume that the D_{2d}, charge-delocalized cation radical corresponds to the transition structure for the HT process. The putative D_{2d} transition structure **6** (Figure 3) is 3.1 kcal/mol higher in energy than the ground-state C_1 structure **5**. The lengths of the double bonds are both 1.366 Å. Surprisingly, a harmonic vibrational

(23) (a) Salhi-Benachenhou, N.; Engels, B.; Huang, M.; Lunell, S. *Chem. Phys.* **1998**, *236*, 53 and references therein. (b) Merer, A. J.; Schoonveld, L. *Can. J. Phys.* **1969**, *47*, 1731. (c) Köppel, H.; Domcke, W.; Cederbaum, L. S.; von Niessen, W. *J. Chem. Phys.* **1978**, *69*, 4252. (d) Toriyama, K.; Okazaki, M. *Appl. Magn. Reson.* **1996**, *11*, 47. (e) Toriyama, K.; Okazaki, M. *Acta Chem. Scand.* **1997**, *51*, 167.

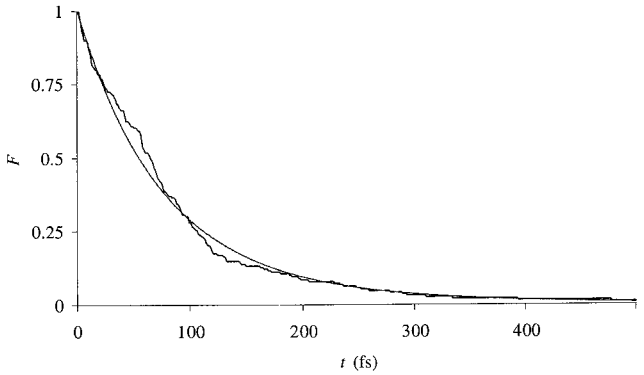

Figure 4. Plot of the fraction of molecules yet to have undergone HT, *F*, versus time (fs) for cation radical **4a** and the monoexponential fit, $F = \exp(-0.01231t)$.

Table 1. Fits to the HT Decay Data for **4a** and **4b** Calculated Using Methods I and II

	monoexponential fit	rms	biexponential fit	rms
		method I		
4a	$F = \exp(-0.01231t)$	0.0049		
4b	$F = \exp(-0.00851t)$	0.043	$F = 0.63\exp(-0.01559t) + 0.37\exp(-0.00397t)$	0.017
		method II		
4a	$F = \exp(-0.00957t)$	0.046	$F = 0.89\exp(-0.01293t) + 0.11\exp(-0.00117t)$	0.018
4b	$F = \exp(-0.00701t)$	0.021	$F = 0.17\exp(-0.01917t) + 0.83\exp(-0.00593t)$	0.015

frequency calculation on the D_{2d} structure revealed it to possess all real frequencies, which implies that it corresponds to a shallow local minimum rather than a transition structure. However, this is an artifact of the theoretical method since the D_{2d} structure, optimized at the AM1-ROHF level, gave a single imaginary frequency, whose vibrational mode corresponded to the transition vector for the HT process.

As the AM1-CI method places the D_{2d}, charge delocalized structure in a local minimum, the lower bound for the activation barrier at this level of theory is 3.1 kcal/mol, and this is probably close to the actual activation energy, given the shallowness of the energy surface in this region.

The Dynamics. Ensembles of 200 trajectories were run for both **4a** and the deuterated system **4b** at 298.15 K. Method I was used to locate the avoided crossing in the calculations, at which point the LZ criterion was applied. The time at which each trajectory was terminated was recorded and curves were plotted for the fraction, *F*, of trajectories remaining after a period of time versus time, *t* (fs), to give an overall decay curve for the HT process. Exponential decay functions were fitted to these curves and the results are presented in Table 1 (Method I). The reciprocals of the exponents of the functions fitted to the decay data are reported as the mean first passage times, τ, for the HT reaction.[24]

Figure 4 shows such a plot for **4a**. A satisfactory monoexponential decay function (eq 5) was fitted to the data with a root-mean-square (rms) value of 0.0049. The calculated τ_h value for HT in **4a** is therefore 8.1×10^{-14} s (298.15 K).

$$F = \exp(-0.01231t) \quad (5)$$

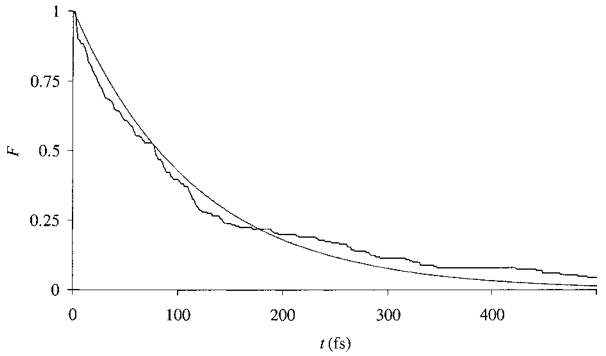

Figure 5. Plot of the fraction of molecules yet to have undergone HT, *F*, versus time (fs) for deuterated cation radical **4b** and best monoexponential fit, $F = \exp(-0.00851t)$.

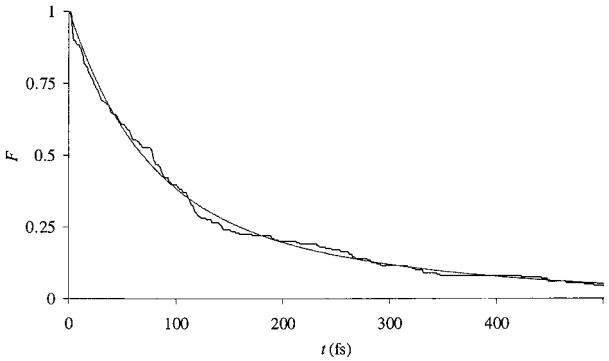

Figure 6. Plot of the fraction of molecules yet to have undergone HT, *F*, versus time (fs) for deuterated cation radical **4b** and the biexponential fit, $F = 63\exp(-0.01559t) + 37\exp(-0.00397t)$.

The best monoexponential fit to the decay of the deuterated cation radical **4b** (eq 6) has a somewhat larger rms value of 0.043 (Figure 5). This gives a τ_d value for HT of 1.2×10^{-13} s.

$$F = \exp(-0.00851t) \quad (6)$$

A better fit to the decay data for **4b** is obtained using the biexponential function,[25] eq 7, with a calculated rms value of 0.017 (Figure 6). The two mean first passage times derived from this fit are $\tau_{d1} = 6.4 \times 10^{-14}$ s and $\tau_{d2} = 2.5 \times 10^{-13}$ s.

$$F = 0.63\exp(-0.01559t) + 0.37\exp(-0.00397t) \quad (7)$$

The charge delocalized D_{2d} structure has strict degeneracy between the ground state and the first excited state; however, not unexpectedly, none of the dynamics trajectories was found to pass exactly through this structure. Indeed, the average magnitude of the electronic coupling V_{el}, estimated to be one-half of the energy gap at the avoided crossing, for the dynamics runs was found to be 0.06 eV for **4a** and 0.07 eV for **4b**. This coupling lies within the adiabatic regime for electron transfer, defined as $V_{el} > k_B T \cong 0.025$ eV at 298.15 K.[26] As a result, many of the trajectories have insufficient kinetic energy in the direction of the avoided crossing to access the upper adiabatic

(24) While it is tempting to equate the reciprocal of our τ values to the corresponding unimolecular rate constants for HT, it is strictly incorrect to do so because the trajectories are halted immediately following HT, without allowing them the opportunity to recross from product well into reactant well. That is, we are assuming infinitely fast deactivation in the product well, whereas dissipation in the reactant well occurs only through dynamics of the atoms. The reciprocal of our τ values would be equal to the unimolecular rate constant in the high-pressure limit (i.e. in solution) if intramolecular vibrational energy redistribution were very much faster than passage over the reaction barrier, but we have no information about that. We are grateful to a referee and to Professor D. G. Truhlar for helpful comments on this point.

(25) *F*-tests performed to compare the relative qualities of the monoexponential and biexponential fits to the decay data for **4b** revealed that the biexponential fit is in fact significantly better at the 95% confidence limit.

(26) Farazdel, A.; Dupuis, M.; Clementi, E.; Aviram, A. *J. Am. Chem. Soc.* **1990**, *112*, 4206.

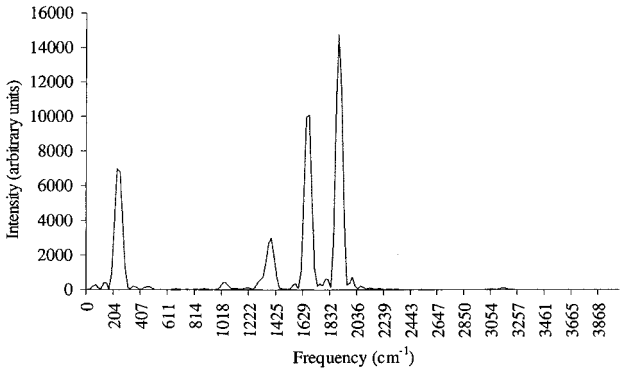

Figure 7. Fourier transform spectrum obtained from the ΔE versus time curve for cation radical **4a**. Four main peaks occur at 224, 1384, 1670, and 1893 cm^{-1}.

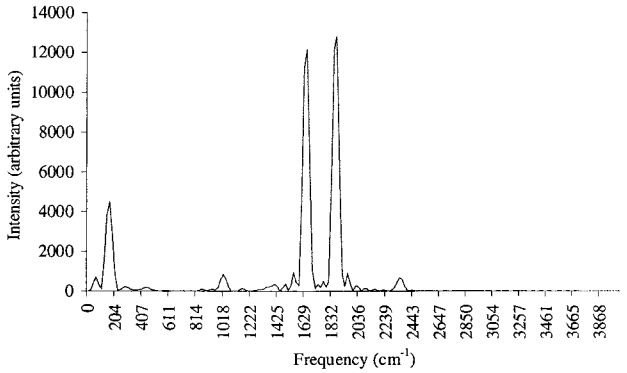

Figure 8. Fourier transform spectrum obtained from the ΔE versus time curve for cation radical **4b**. Three main peaks occur at 163, 1649, and 1873 cm^{-1}.

surface within the avoided crossing region. However, this estimate for the magnitude of the electronic coupling is too high since inspection of the trajectory data revealed that the energy gap associated with the avoided crossing, as determined using Method I, is larger than its minimum value. This problem is circumvented using Method II (vide infra).

Because, within the context of the LZ criterion, the probability of trajectory surface hopping is related to the square of the coupling matrix element V_{el}, the rate of fluctuation of the energy gap, ΔE, between the ground state and the first excited state as the trajectory progresses should give an indication of the rate at which the avoided crossing is encountered and, therefore, an indication of the rate of hole transfer. To delineate which molecular vibrations are important contributors to the energy gap fluctuation, a single trajectory for each system was run and a Fourier transform (FT) of ΔE versus t was taken to give intensity (arbitrary units) versus frequency (cm^{-1}).[27] The total kinetic energy assigned to the normal vibrational modes was set to be less than the minimum energy required to access the avoided crossing region. Each vibrational mode was assigned equivalent amounts of kinetic energy (i.e. equal amounts of quanta were assigned to each mode). The restriction of the trajectory to the reactant well is necessary because if the trajectory were allowed to move between the reactant and product wells the resulting FT spectrum becomes complicated, owing to the drastic changes to several of the vibrational force constants that take place upon traveling through the avoided crossing region. Each trajectory was run for 500 fs, with time intervals of 0.1 fs. A Fast Fourier Transform was used, giving a resolution of approximately 20 cm^{-1}. Figures 7 and 8 show the FT spectra of intensity (arbitrary units) versus frequency (cm^{-1}) obtained from the ΔE versus time plot for **4a** and **4b**, respectively.

The resulting FT spectrum for **4a** displays four major peaks (Figure 7), at 224, 1384, 1670, and 1893 cm^{-1}. These peaks could be correlated with calculated normal harmonic vibrational modes (ν_h) for the optimized ground-state geometry of **4a**. The 1893 and 1670 cm^{-1} peaks were assigned to the stretching modes of the two-electron π bond ($\nu_h = 1894$ cm^{-1}) and the charge localized, one-electron π bond ($\nu_h = 1659$ cm^{-1}). The 224 cm^{-1} peak corresponds to the torsional mode of the terminal CH_2 group about the charge localized one-electron π bond ($\nu_h = 235$ cm^{-1}), and the fourth peak at 1384 cm^{-1} corresponds to CH bending distortions occurring in the CH_2 groups and the hydrocarbon cage. The latter peak is much less intense than the other three peaks, and therefore this vibrational mode plays only a minor role in bringing the trajectory to the avoided crossing.

The FT spectrum for the deuterated species **4b** (Figure 8) displays three main peaks, at 163, 1649, and 1873 cm^{-1}, and these correspond respectively to torsion and stretching modes of the double bonds, as described above for **4a**. A fourth, minor peak occurring at 1000 cm^{-1} corresponds to the 1384 cm^{-1} peak in the FT spectrum for **4a**. It can be seen that replacing the methylene protons with deuterium reduces the significance of the effects of the CH/CD bending distortions in this vibrational mode to such a point that they barely contribute to the modulation of ΔE.

The MD-TSH calculations on **4a** and **4b** provide insight into the role played by nuclear vibrations on the dynamics of the HT process. Comparing the mean first passage times in **4a** and **4b** obtained from the monoexponential fits, it is predicted that HT should occur more rapidly in the former system. An approximate kinetic isotope effect can be calculated by taking the ratios of the mean first passage times for **4b** and **4a** ($k_h/k_d \cong \tau_d/\tau_h$), giving a value of 1.45.[28] Although the significant approximations involved in the calculations suggest that the absolute magnitudes of the rate constants should not be considered reliable, a rough cancellation of errors can be expected in the rate constant ratio that defines the isotope effect, and so its magnitude may be more trustworthy.

From the FT spectra of **4a** and **4b**, it is seen that the ratios of the magnitudes of the corresponding π bond stretching frequencies for **4a**:**4b** are small: 1.02 for the two-electron π bond and 1.03 for the one-electron π bond. The ratio of the frequencies of the torsional modes for **4a**:**4b** is 1.41. The similarity of the magnitude of this ratio to the k_h/k_d isotope effect indicates that the isotope effect is due largely to the torsional mode, and not to the double bond stretching vibrations. This is to be expected since the latter vibrations are barely influenced by H/D substitution. That the magnitude of the isotope effect should depend on a ratio of related vibrational frequencies in the isotopic variants rather than the usual exponential of the difference in frequencies derives from the fact that this isotope effect has a fundamentally different origin from those observed in most reactions. Rather than being due to a change in effective barrier height, caused by differences in zero-point energy, this isotope effect derives from a change in encounter frequency with the seam of avoided crossings.

(27) Osguthorpe, D. J.; Dauber-Osguthorpe, P. *J. Mol. Graphics* **1992**, *10*, 178.

(28) Although the decay data for **4b** are expressed more precisely by a biexponential function, the kinetic isotope effect for HT between **4a** and **4b** is calculated by using the rate constant obtained from the monoexponential fit to the decay data for **4b**. Errors introduced by using this fit are assumed to be small.

If we consider the FT spectra for **4a** and **4b**, it is intuitively obvious that the π bond stretching modes will be of primary importance in bringing the trajectories to the avoided crossing region, and that these modes should be more or less 180° out of phase with respect to each other. This is necessary because the two double bonds must have nearly identical lengths at the avoided crossing (i.e. the charge is delocalized over both double bonds). However, this is only a necessary, but not sufficient condition for HT to occur, since the avoided crossing must also be associated with a nonzero value of V_{el}. This is not the case for the putative D_{2d} transition structure. Consequently, the successful trajectories which effect the HT process are associated with symmetry-breaking deformations of the methylene groups, particularly torsional modes, as evidenced by the FT spectra.

An interesting point revealed by the MD-TSH simulations is that the decay data for HT of **4a** are well expressed by a monoexponential function, eq 5, whereas that for the deuterated system **4b** is expressed more satisfactorily by a biexponential function, eq 7. τ_{d1} for HT in **4b** which is associated with the larger preexponential factor ($\tau_{d1} = 6.4 \times 10^{-14}$ s) is comparable in magnitude to τ_h for HT in **4a** ($\tau_h = 8.1 \times 10^{-14}$ s), whereas τ_{d2} associated with the minor preexponential factor is about three times larger ($\tau_{d2} = 2.5 \times 10^{-13}$ s). This suggests that two different populations (63:37) are present in the initial canonical ensemble of **4b**, which do not interconvert by vibrational energy redistribution processes during the dynamics runs.

Indeed, we have noted that, owing to the isotope effect, the vibration associated with torsion about the one-electron π bond is associated with more quanta (n_i) for **4b** than for **4a**. Thus, inspection of the canonical ensembles determined at 298.15 K revealed that for **4a** 52% of the trajectories were initialized with only ZPE in this vibrational mode and that the remaining 48% were initialized with one extra vibrational quantum of energy ($n_i = 1$) in the same mode. In contrast, for **4b**, a significant fraction of trajectories (24%) were initialized with two vibrational quanta ($n_i = 2$) in the torsional mode. Analysis of the individual trajectories for **4b** reveals that most of those which possessed two quanta in the torsional vibration were associated with a greater degree of twisting about the one-electron π bond than those which were associated with fewer quanta. Consequently, the former set of trajectories were spending more time in regions of the potential energy surface which are not conducive to the HT process. It is probably these trajectories which make the major contribution to τ_{d2} (eq 7). For $n_i < 2$, the amplitude of the torsional mode is smaller than that for $n_i = 2$, and the HT rate is therefore faster. Since all trajectories for **4a** were initialized with $n_i < 2$ in the torsional mode associated with the one-electron π bond, the dynamics for this molecule are now well represented by a monoexponential fit.

The Dependence of the Dynamics on the Choice of Method for Locating the Avoided Crossing. So far, we have used Method I, namely the onset of hole transfer on the lower adiabatic PES (as judged by charge migration), as the criterion for locating the avoided crossing. To assess the sensitivity of our MD-TSH procedure to the criterion used for locating the avoided crossing, we have repeated our MD-TSH calculations but using Method II as the criterion; that is, the Landau−Zener calculation is carried out every time the plot of energy gap vs time passes through a minimum. Ensembles of 200 trajectories were run for both **4a** and **4b** at 298.15 K and the calculated rate data are presented in Table 1.

Comparison of the exponents from monoexponential fits to the decay curves shows that those for **4a** and **4b** using Method II are respectively about 22% and 18% smaller than those using Method I (i.e., the τ values calculated using Method II are increased). For both **4a** and **4b**, the average value of one-half of the energy gap between the two adiabatic surfaces at the avoided crossing located using Method II is 0.01 eV and is about six times smaller than that calculated from the avoided crossing located using Method I (0.06 eV). Since Method II locates the minimum value for the energy gap, then the value of the electronic coupling, V_{el}, for the HT process is 0.01 eV, rather than the larger value of 0.06 eV estimated using Method II. From a dynamics point of view HT for both **4a** and **4b** is predicted to occur nonadiabatically. That Method II gives larger τ values than Method I for both **4a** and **4b** is due to the fact that the energy gap associated with the avoided crossing is larger using Method I than using Method II. Consequently, slightly more trajectories are undergoing TSH using Method II, compared to using Method I.

The approximate secondary kinetic isotope effect (k_h/k_d) calculated using Method II is 1.37, and is 5.5% smaller than that calculated using Method I. This value is still in reasonable agreement with the calculated ratio (1.41) of the frequencies for the torsional mode about the one-electron π bond for **4a** and **4b**.

In summary, from a qualitative point of view, the calculated τ values for HT and the kinetic isotope effects for **4a** and **4b** are not particularly sensitive to the choice of method used for locating the avoided crossing. However, we feel that Method II is superior to Method I since it locates the minimum value for the energy gap and therefore maximizes the probability of TSH.

IV. Conclusion

Several experimental observations of rapid, symmetry forbidden, electron and excitation energy transfer have been reported, including photoinduced electron transfer in **1**[3b] and energy transfer in systems based on **3**.[10b] Of particular interest here is the observation of photoinduced ET in **2**, which takes place from the locally excited Ru(II) donor to the Os(III) acceptor.[10a] Thermal HT in the bismethyleneadamantane systems, **4a** and **4b**, provide a simple model of the symmetry forbidden electron-transfer process observed in **2**. While the observed rate data for **2** cannot be directly compared with the calculated HT rates for **4a** and **4b**, useful insight into the symmetry forbidden processes may be obtained.

The calculated kinetic isotope effect for **4a** and **4b** at 298.15 K shows that, although antisymmetric stretching of the double bonds is necessary to facilitate HT, symmetry breaking torsional $CH_2(CD_2)$ modes, associated largely with the one-electron π bond, play an important role in the HT dynamics. Rapid electron transfer observed in **2** could presumably be attributed to similar symmetry breaking, vibronic effects.

Altering the method used to locate the avoided crossing has little qualitative effect on the mean first passage time for HT and kinetic isotope effects, although that based on locating the minimum energy gap between the adiabatic surfaces is preferable to that based on detecting charge shift since it maximizes the TSH probability.

Our MD-TSH method has allowed a qualitative description of the nature of HT dynamics in the bismethyleneadamantane cation radical, which is entirely consistent with intuition. We are therefore confident that application of our method to more complex molecular systems of chemical interest will produce useful and qualitatively reliable insights into subtle nuclear dynamic factors affecting ET and HT processes.

Acknowledgment. We gratefully thank the Australian Research Council (ARC) for support of this work. The awards of an ARC Senior Research Fellowship (to M.N.P-R.) and an ARC postgraduate award (to G.A.J.) are gratefully acknowledged. Furthermore, we thank the New South Wales Centre for Parallel Computing for generous allocation of computer time on their Silicon Graphics Power Challenge.

JA9917823